Pergamon

Bioorganic & Medicinal Chemistry, Vol. 5, No. 8, pp 1519–1529, 1997

PII: S0968-0896(97)00101-6
0968-0896/97 $17.00 + 0.00

Chemical Model Studies on the Monoamine Oxidase-B Catalyzed Oxidation of 4-Substituted 1-Methyl-1,2,3,6-tetrahydropyridines

Christelle Franot, Stéphane Mabic and Neal Castagnoli, Jr.*
Department of Chemistry, Virginia Tech, Blacksburg, VA 24061-0212, U.S.A.

Abstract—The MAO-B catalyzed α-carbon oxidation of amines has been proposed to proceed via either a single electron transfer (SET) or hydrogen atom transfer (HAT) pathway. In an attempt to distinguish between these pathways, we have examined the α-carbon oxidation of a series of 4-substituted 1-methyl-1,2,3,6-tetrahydropyridine derivatives, compounds which are MAO-B substrates, employing chemical models of the SET pathway [using the PF_6^- salt of Fe^{+3} (1,10-phenanthroline)$_3$ as the electron acceptor] and HAT pathway (using the *tert*-butoxyl radical as the hydrogen atom acceptor). The rates of oxidation and deuterium isotope effects observed with these compounds were similar with the two model reactions. Consequently, unlike their utility in modeling the related cytochrome P450 catalyzed α-carbon oxidation of *N,N*-dimethylaniline derivatives, it appears that these reagents will not distinguish between the proposed pathways. © 1997 Elsevier Science Ltd.

Introduction

The flavoenzymes monoamine oxidase (MAO)-A and -B catalyze the oxidative *N*-dealkylation of a variety of amines including neurotransmitters such as dopamine and serotonin.[1–4] Several mechanisms have been proposed for the MAO-B catalytic pathway[5,6] with the most attention having been given to one based on an initial single electron transfer (SET) step (path **A**, Scheme 1) from the parent amine (**1**) to the oxidized flavin (FAD) followed by deprotonation of the resulting aminyl radical cation **2** to form the radical intermediate **3**.[7–10] A second electron transfer from **3** to FADH• yields the imine product **4** and $FADH_2$. This proposal is supported by the mechanism-based inactivator properties of compounds such as benzylcyclopropylamine (**5**).[11,12] The inactivation of MAO-B presumably proceeds via rapid ring opening of the SET-generated cyclopropylaminyl radical cation **6** to form the primary carbon radical **7** that covalently modifies an active site functionality (Scheme 2). An alternative hydrogen atom transfer (HAT) pathway (path **B**) has been proposed for this reaction since ΔG for the electron transfer step is estimated to be much larger than the experimentally determined ΔG° for the anaerobic reduction of FAD by benzylamine.[13]

Our mechanistic studies on the MAO-B catalytic pathway have focused on 1,4-disubstituted 1,2,3,6-tetrahydropyridine derivatives.[14,15] A wide variety of 4-substituted 1-methyltetrahydropyridine analogues (**I**, see Chart 2) undergo MAO-A and MAO-B catalyzed oxidization to the corresponding iminium (dihydropyridinium) metabolites (**II**) with V_{max}/K_m values as high as 4151 min^{-1} mM^{-1}.[16a] Consistent with the SET pathway, some 1-cyclopropyltetrahydropyridine analogues (**8–10**, Chart 1) are good MAO-B inactivators.[15,17] Other analogues, however, are poor inactivators and good substrates (**11** and **12**)[15,18] or substrates only (**13** and **14**).[19] Since cyclopropylaminyl radical cations are likely to ring open at extremely rapid rates,[20] the efficient

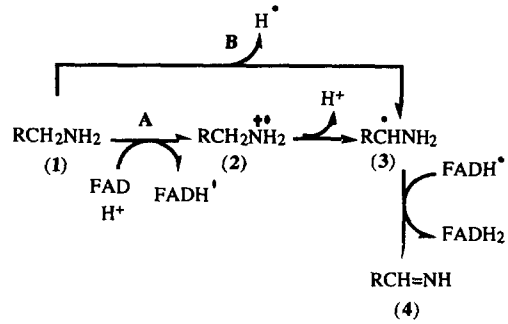

Scheme 1. SET and HAT pathways proposed for the MAO-B catalyzed oxidation of amines.

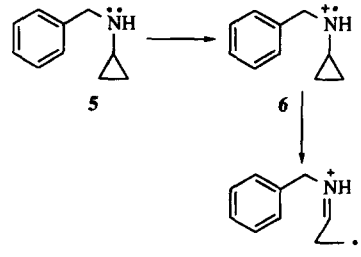

Scheme 2. Pathway proposed to account for the inactivation properties of benzylcyclopropylamine (**5**).

*Department of Chemistry, Virginia Tech, Blacksburg, VA 24061-0212, U.S.A. Telephone: (540) 231-8202; fax: (540) 231-8890; e-mail: ncastagnoli@chemserver.chem.vt.edu

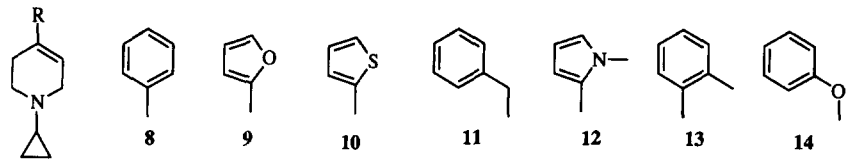

	8	9	10	11	12	13	14
V_{max}/K_m:	TS[a]	TS[a]	TS[a]	2025	290	630	1650
k_{inact}/K_i:	3.85	TF[b]	TF[b]	0.06	GS/PI[c]	SO[d]	SO[d]

[a]TS = too slow to measure. [b]TF = too fast to measure. [c]GS/PI = good substrate and poor inactivator properties prevented estimate of k_{inact}/K_i. [d]SO = substrate only.

Chart 1. 1-Cyclopropyltetrahydropyridine derivatives displaying MAO-B substrate/inactivator properties.

turnover observed was interpreted as evidence in support of partitioning of these cyclic tertiary allylamines between the SET and HAT pathways. A normal deuterium isotope effect on the rate of oxidation of **11** and essentially no isotope effect on the rate of inactivation of MAO-B by **11** was viewed as being consistent with this proposal.[18]

A debate, similar to that described above for MAO-B, has focused on the cytochrome P450 catalyzed oxidation of amines.[21] Recently, Dinnocenzo reported evidence suggesting that the cytochrome P450 catalyzed oxidative deamination of various substituted *N,N*-dimethylaniline derivatives proceeds by an HAT and not SET pathway.[22] This conclusion was based on the observation that the deuterium isotope effect profile for the enzyme catalyzed reactions was similar to that of a chemical model for the HAT pathway but different from that of a chemical model for the SET pathway. In this manuscript we report the results of our initial efforts to carry out an analogous deuterium isotope effect profile study on MAO-B by examining the rates of oxidation of several 4-substituted 1-methyltetrahydropyridine analogues **I** (**15–21**, Chart 2) to the corresponding dihydropyridinium metabolites **II** (**22–28**) using chemical models of the HAT and SET pathways. Estimates of the deuterium isotope effects on these conversions were obtained with the monodeuterated analogues **I-d_1** (**15-d_1–19-d_1**). Included in this group are compounds with excellent to very poor MAO-B substrate properties.

Results and Discussion

Chemistry

The syntheses of the test tetrahydropyridine derivatives (Structures **I**, Chart 2) have been reported previously (see the Experimental section for citations). Estimations of the deuterium isotope effects required the corresponding **6-d_1** analogues **I-d_1**, which were prepared by $NaBD_4$ reduction of the dihydropyridinium intermediates **II**. The preparation of **II**[16b,23,24] proceeded by a Polinovski-type reaction[25] involving the *m*-chloroperoxybenzoic acid (*m*-CPBA) oxidation of the undeuterated tetrahydropyridines **I** followed by reaction of the resulting *N*-oxides **III** (**29–35**) with trifluoroacetic anhydride (TFAA, Scheme 3). For the most part the syntheses of the dihydropyridinium intermediates proceeded as described in the cited literature. The deuterium enrichments, estimated by gas chromato-

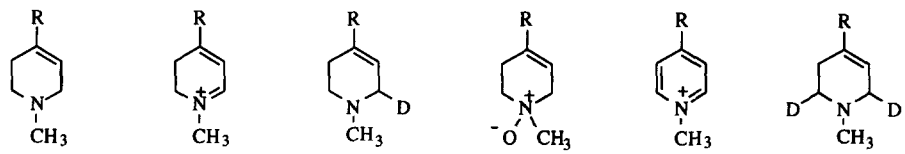

	I	II	I-d_1	III	IV	I-d_2	
R	C_6H_5	NCH3	OC_6H_5	$C(CH_3)_3$	SC_6H_5	N	$COOCH_3$
I	15	16	17	18	19	20	21
V_{max}/K_m[a]	1431[15]	1790[15]	4151[16a]	92[43]	3425[16b]	6[15]	?
II	22	23	24	25	26	27	28
I-d_1	15-d_1	16-d_1	17-d_1	18-d_1	19-d_1	20-d_1	21-d_1
III	29	30	31	32	33	34	35
IV	36	37	38	39	40	41	42
I-d_2	15-$d2$	16-d_2	17-d_2	18-d_2	19-d_2	20-d_2	21-d_2

[a]Measured at 37 °C.

Chart 2. Structures of compounds examined in the SET and HAT chemical models.

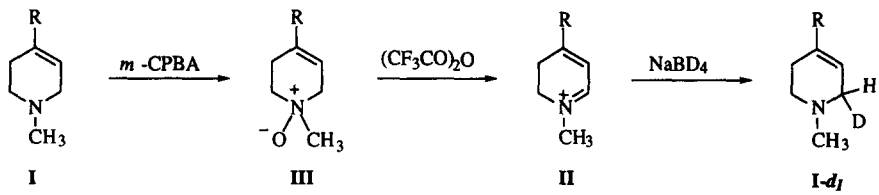

Scheme 3. Synthesis of tetrahydropyridine-**6-*d*1** substrates **I-*d*1**.

graphy-electron ionization mass spectroscopy (GC-EIMS) analysis (see below), were >97% except for analogues **20-d_1** and **21-d_1**, which were only about 90% deuterium enriched. We speculate that in these cases deuterium exchange occurs through the tautomeric forms **43** and **44** (Scheme 4). Isotope effect measurements were not performed on these two compounds.

The synthesis of the 1-methyl-4-(1-methyl-2-pyrrolyl)-2,3-dihydropyridinium intermediate ***23*** was approached by an analogous sequence (Scheme 5) only starting from the piperidinol ***46*** as previously reported.[26] Treatment of the *N*-oxide **47** with TFAA gave a yellow solid with λ_{max} = 409 instead of 421 nm as reported for **23**. The ^{1}H NMR spectrum displayed signals expected for the *N*-methyl (3.68 ppm) and dihydropyridinium (7.34–7.37 and 8.64–8.66 ppm) protons. Two doublets at δ 6.83 and 6.97 ppm were tentatively assigned to the β-pyrrolyl proton signals. The signal for the C-5 pyrrolyl proton, however, expected near 7.4 ppm, was absent. Treatment of this unstable compound with $NaBH_4$ gave two products with nominal masses *m/z* 272 and *m/z* 274 as estimated by GC-EIMS. The corresponding $NaBD_4$ reduction products had nominal masses *m/z* 273 and *m/z* 276. Based on these data, we propose the 5-trifluoroacetyl derivative **49** as the principal product of the reaction between the piperidinol *N*-oxide **47** and TFAA. Partial reduction (iminium group only) or complete reduction (iminium and carbonyl groups) of **49** with $NaBH_4$ would generate **50** ($M^{\bullet+}$ 272 Da) and **51** ($M^{\bullet+}$ 274 Da) or, with $NaBD_4$, **50-d_1** ($M^{\bullet+}$ 273 Da) and **51-d_2** ($M^{\bullet+}$ 274 Da) (see the Experimental section for details). The formation of **49** presumably proceeds via the trifluoroacetylated intermediate **48**. When the less nucleophilic tetrahydropyridine **16** was used, the reaction proceeded smoothly via the *N*-oxide **30** to yield the dihydropyridinium intermediate **23** which was reduced to the desired **16-d_1** (Scheme 5).

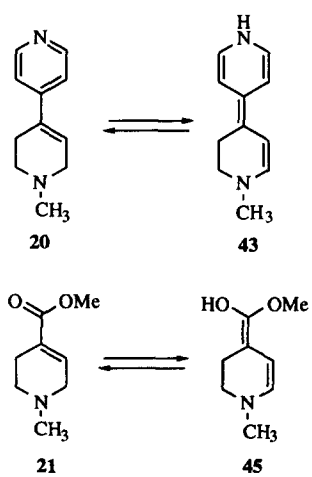

Scheme 4. Tautomeric forms of **20** and **21**.

Chemical model studies

The PF_6^- salt of the Fe^{3+}(1,10-phenanthroline)$_3$ [Fe^{+3}(Phen)$_3$] complex, a powerful single electron oxidant, was used in the SET model. The redox potential of the $Fe^{+3}(Phen)_3/Fe^{+2}(Phen)_3$ couple is +1.10 V (versus standard hydrogen potential),[27] well above the reported oxidation potential of cyclic tertiary amines.[28] The proposed SET pathway is illustrated in Scheme 6 with 1-methyl-4-phenyl-1,2,3,6-tetrahydropyridine (**15**) as the substrate. The oxidation proceeds through initial SET to generate the aminyl radical cation **52** which, following deprotonation, yields the carbon radical **53** that is oxidized further by the Fe^{+3} reagent to yield the dihydropyridinium product **22**. A second 2-electron oxidation converts **22** to the stable pyridinium product **36**. Therefore, 4 Fe^{+3} equiv are require to oxidize **15** to **36**. Pyridine was used to deprotonate the expected aminyl radical cation intermediate **52** because of its moderate basicity and high oxidation potential (+1.82 V versus silver –0.1 M $AgClO_4$).[29] The reaction was followed by GC-EIMS after reduction with $NaBD_4$ and extraction with Et_2O. Under these conditions, the expected dihydropyridinium and pyridinium species, **22** and **36**, respectively, are reduced to **15-d_1** and **15-d_2** which can be measured by GC-EIMS (Scheme 6).

We initially conducted the SET model reactions in CH_2Cl_2. The Fe^{+3} reagent, however, was only partially soluble in this solvent and the reaction was very sluggish. Both the dihydropyridinium (**22**) and pyridinium (**36**) species were detected in all samples analyzed during the 24 h reaction period, even when only 2 equiv of the [Fe^{+3}(Phen)$_3$] complex were used. Although the formation of **36** may be mediated by [Fe^{+3}(Phen)$_3$] oxidation of the free base **54**,[30] an alternative pathway would involve a redox (disproportionation) reaction between the dihydropyridinium species **22** and its conjugate base **54**, a pathway which has been described previously.[31] This possibility was investigated by examining the [Fe^{+3}(Phen)$_3$] oxidation of a mixture of three parts **15** and seven parts **15-d_4**. The higher concentration of **15-d_4** was used to take into account an

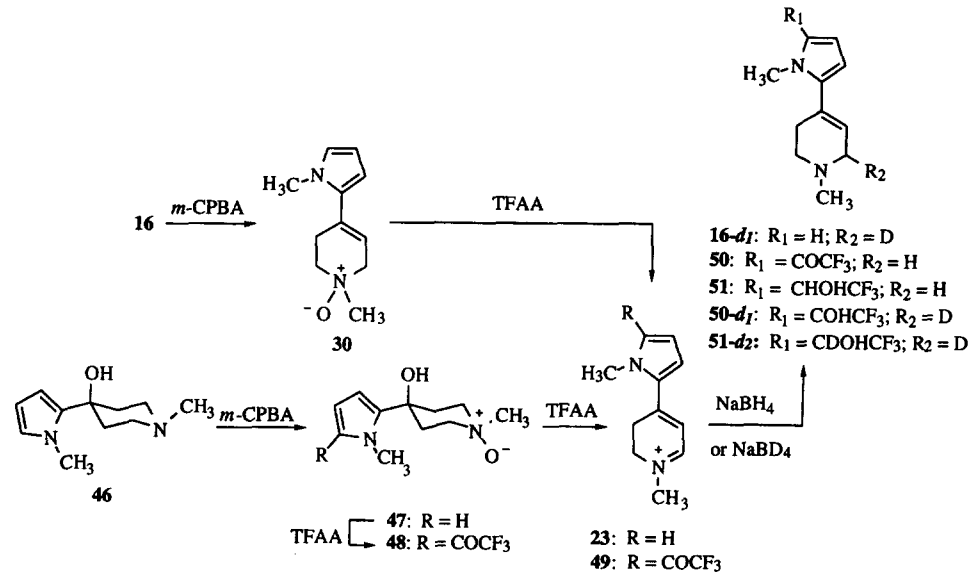

Scheme 5. Reaction pathways encountered with the pyrrolyl derivatives **16** and **46**.

anticipated deuterium isotope effect on the disproportionation reaction. As illustrated in Scheme 7, disproportionation between **54-d_0** (derived from **22**) and **22-d_3** (derived from **15-d_4**) would lead to the formation of **15-d_3**. GC-EIMS analysis of this reaction mixture showed that 17% (5 min) and 29% (45 min) of **15-d_4** was converted to **15-d_3**. We conclude, therefore, that disproportionation is a major source of the pyridinium species formed under these reaction conditions, a complication that compromises the intended kinetic studies of this reaction.

The $[Fe^{+3}(Phen)_3]$ complex was more soluble and the reaction rates faster in MeCN than in CH_2Cl_2. As in CH_2Cl_2, on addition of **15**, the blue color of the $[Fe^{+3}(Phen)_3]$ complex immediately changed to red which is indicative of the reduction of Fe^{+3} to Fe^{+2}. With 3 equiv of the $[Fe^{+3}(Phen)_3]$ complex, 1 mM **15** was completely oxidized to the dihydropyridinium species **22** within 10 min without any detectable formation of the pyridinium species **36**. Consequently, disproportionation does not appear to take place under these conditions. The stability of synthetic **22** in MeCN was confirmed since repeated ^1H NMR scans over an hour showed signals of the starting material only. With reaction times greater than 30 min, **15-d_2**, the product formed from the $NaBD_4$ reduction of the pyridinium species **36** (Scheme 6), also was observed in the GC-EIMS tracing. As expected, with 4 equiv or more of the Fe^{+3} reagent, **15** was completely converted to the pyridinium species **36**. Since disproportionation no longer complicated the reaction scheme, MeCN was used in subsequent studies.

The HAT model employed the *tert*-butoxyl radical (*t*-BuO•) generated from *tert*-butyl peroxybenzoate in the presence of a catalytic amount of CuCl. This perester reaction, first described by Karasch and Fono,[32] has been applied successfully to effect hydrogen atom abstraction from compounds bearing a variety of

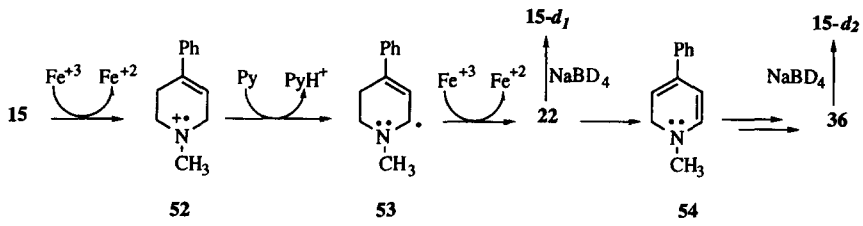

Scheme 6. SET pathway for the oxidation of MPTP (**15**).

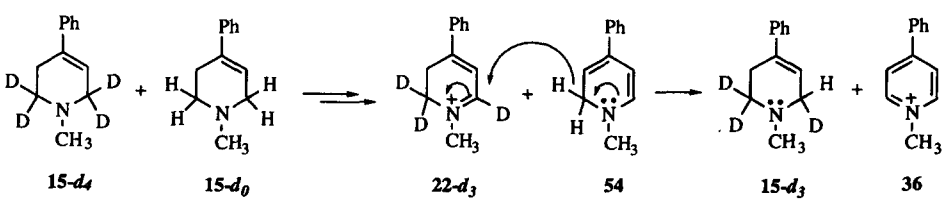

Scheme 7. Disproportionation pathway proposed for dihydropyridinium species derived from a mixture of deuterated and undeuterated MPTP.

functionalities.[33] Mechanistic studies suggest a three-part reaction sequence,[34] which is illustrated in Scheme 8 with **15** as substrate. Step 1 (electron transfer from CuCl) gives *t*-BuO• and the cupric chloride salt of benzoic acid. Step 2 (H• transfer) generates the allylic radical **53** which, in step 3, is oxidized to the dihydropyridinium product **22**. Although **15** contains two types of allylic protons, abstraction of the allylic proton α to the amino group should be more favored because of the stabilization by the tertiary amine. This was confirmed by semiempirical calculations (AM1) that give a 11.83 kcal/mol difference in the heats of formation of the two possible allylic radicals in favor of the radical **53**. Literature reports state that the first step of the reaction is instantaneous and shows no inductive period.[35]

Treatment of **15** at room temperature in MeCN with 2 equiv of *tert*-butyl peroxybenzoate and a catalytic amount of CuCl was followed by $NaBD_4$ workup of the reaction mixture and by GC-EIMS analysis. The reaction was monitored for the next 10 min. The quantitative conversion of the starting material to the corresponding pyridinium species was documented by ^1H NMR analysis, which showed signals for **36** but not for **15** or **22**, and by GC-EIMS analysis following $NaBD_4$ reduction which showed the expected fragment ion at *m/z* 98 derived from **15-*d*$_2$**. The reaction did not go to completion with less than 2 equiv of oxidizing agent but apparently no dihydropyridinium was present since no evidence for **15-*d*$_1$** could be detected by GC-EIMS analysis following $NaBD_4$ work-up.

In parallel to the SET model, conversion of the dihydropyridinium intermediate to the final pyridinium product could proceed by disproportionation or via *t*-BuO• mediated oxidation of the 1,2-dihydropyridine species **54** formed by benzoate deprotonation of **22**. An experiment similar to the one described for the SET model was run to evaluate the possible contribution of the disproportionation reaction to pyridinium formation. The perester reaction was performed with a 3/7 mixture of **15-*d*$_0$/15-*d*$_4$** and formation of **15-*d*$_3$** was monitored by GC-EIMS after hydrolysis of the reaction mixture at various times. Since there was no evidence for the presence of **15-*d*$_3$**, we conclude that disproportionation is unlikely to contribute significantly to pyridinium formation in this reaction. The absence of disproportionation may be a consequence of the ease with which **54** is converted to **55** due to the resonance stabilization of the **55**. Using semiempirical calculations (AM1), the heat of formation of compound **53** from **15** was found to be greater (6.68 kcal/mol) than the heat of formation of compound **55** from the dihydropyridine **54** (1.53 kcal/mol). Consequently, abstraction of the allylic hydrogen of **54** may be faster than the disproportionation process as might be predicted from the published observations on the relative reactivity of radicals **53** and **55** with a number of molecules of biochemical interest.[36] The reactions were always faster with **53** than with **55**, consistent with the greater stability of **55**.[37]

Oxidation rates

The rates of oxidation of the tetrahydropyridine derivatives under SET model reaction conditions were too fast to monitor accurately by the GC-EIMS assay. Consequently, in order to estimate the influence of the C4-substituent on the rates of oxidation in the SET model, relative oxidation rates were determined. Substrate **15** was taken as a reference whenever possible. Equimolar quantities of two tetrahydropyridine derivatives were examined in the presence of only 1.8 equiv of $[Fe^{+3}(Phen)_3]$ and pyridine so that, during the subsequent 15 min, the two substrates were partially converted to the corresponding dihydropyridinium species. No evidence of pyridinium formation was noted under these conditions. The relative rates (k_A/k_B) of oxidation of the two substrates A and B were calculated from equation 1 in which $[T_A]$ and $[T_B]$ represent the concentrations of the tetrahydropyridine derivatives A and B at times 0 and 15 min. The concentrations at 15 min were estimated by GC-EIMS analysis of the reaction mixtures which had been quenched with $NaBD_4$. The rate of oxidation of 1-methyl-4-(1-methyl-2-pyrrolyl)-1,2,3,6-tetrahydropyridine (**16**) was compared to that of 1-methyl-4-(4-pyridyl)-1,2,3,6-tetrahydropyridine (**20**) and then related to MPTP because the GC retention times of **15** and **16** overlapped.

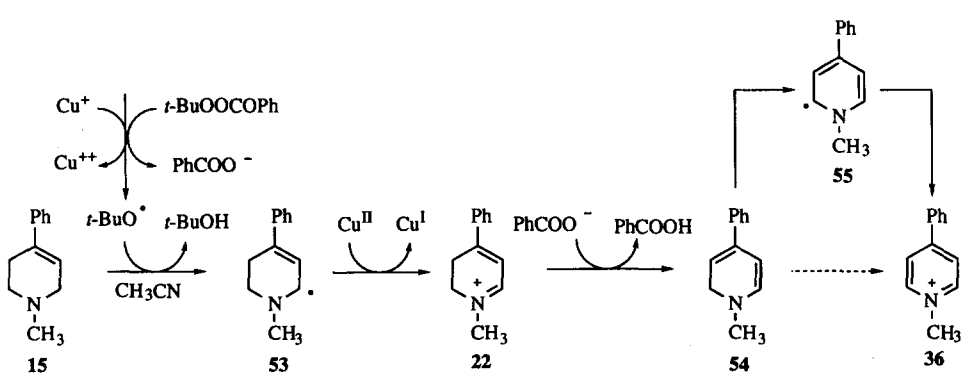

Scheme 8. Proposed hydrogen abstraction mechanism.

$$\frac{k_A}{k_B} = \ln \frac{[T_A]_{15}/[T_A]_0}{[T_A]_{15}/[T_B]_0} \quad (1)$$

The rates of oxidation of the tetrahydropyridine derivatives to the corresponding pyridinium products under HAT model reaction conditions using 5 equiv of *tert*-butyl peroxybenzoate were monitored by GC-EIMS following $NaBD_4$ reduction of timed aliquots. Plots of the natural logarithm of the concentrations of the starting tetrahydropyridine as a function of time gave straight lines during the first 10 min of all reactions. The rates of substrate oxidation were then calculated from these pseudo first-order rate plots.

The results of these studies (Table 1) show no clear trend. The values observed with the HAT model reaction, which parallel somewhat the enzyme catalyzed reaction, suggest that this reaction is facilitated by C-4 electron donating groups, possibly through stabilization of the allylic radical intermediate. The relatively low value for the 4-phenoxy analogue **17** in the model reaction, however, is not consistent with the trend observed in the enzyme-catalyzed reaction. The relative rates observed in the SET model reaction are quite similar to each other with the exception of the pyrrolyl compound **16**. Consequently, electronic effects may have less influence on the SET pathway than is the case with the HAT pathway. It should be pointed out that analytical problems forced us to estimate the relative rate of oxidation of **16** indirectly and therefore this value may be less reliable. With the available rate data we conclude that it is not possible to make a clear distinction between the two pathways.

Isotope effects

An isotope effect study was undertaken to evaluate further the potential utility of these chemical models to distinguish between the proposed SET and HAT enzyme catalyzed pathways. In these reactions, the tetrahydropyridine-6-d_1 analogues (**I-d_1**) served as substrates. As reported above, compounds **20** and **21** were not included because of poor (90%) deuterium enrichment. In order to increase the data base, we included the 4-*tert*-butyl (**18**) and 4-thiophenoxy (**19**) analogues in this experiment. The experimental design involved treatment of the oxidized products (**II/II-d_1** and **IV/IV-d_1**) with $NaBH_4$ and GC-EIMS selected ion monitoring to determine the deuterium content of the resulting tetrahydropyridines (**I/I-d_1**) as shown in Scheme 9. Reactions were conducted over a 12-h period with a 10 mol excess of the oxidizing agent to insure that all starting material was consumed before treatment with $NaBH_4$. The completeness of each reaction was confirmed since GC-EIMS analysis of reaction mixture aliquots worked-up prior to the addition of $NaBH_4$ showed no starting material. In the case of the pyrrolyl analogue **16**, only 4 equiv of oxidizing agent were used in the SET model reaction because of apparent complexation of the substrate with the iron reagent. The isotope effects were defined as the d_0/d_1 ratios of the tetrahydropyridine products isolated after treatment of the reaction mixture with $NaBH_4$.

Small, normal isotope effects (1.65–2.30), characteristic of a nonsymmetrical transition state,[38] were observed with both the SET and the HAT chemical models (Table 2). These results point to the importance of carbon–hydrogen bond cleavage in the SET deprotonation step as expected on the basis of the normal isotope effect observed for the chemical deprotonation of a purified *N*-methylanilinium radical cation reported by Dinnocenzo and Bannach.[39] The influence of the 4-substituent on the transition state as revealed by these data seems to be very small since the isotope effects measured are not very different. Consequently, as with the results of the rate studies summarized in Table 1, it appears that the differences in isotope effects will be too small to allow us to distinguish between the SET and HAT pathways. Work is in progress to extend these efforts to examine the reactivities of various 4-substituted 1-cyclopropyl-1,2,3,6-tetrahydropyridine derivatives which have been characterized as either good substrates or good inactivators of MAO-B.

Table 1. Rates of oxidation of **15**, **16**, **17**, **20**, and **21** by the SET and HAT chemical models and by MAO-B

C-4 substituent		$k_{relative}$ (SET)[a]	k_{obs} (min^{-1}) (HAT)[a]	k_{obs} (min^{-1} mM^{-1}) (MAO-B)[c]
Ph	**15**	1	0.199 ± 0.011 (1.0)[b]	1400 (1.0)[b]
	**16**	9.00 ± 1.00	0.258 ± 0.030 (1.3)	1800 (1.3)
–OPh	**17**	1.94 ± 0.08	0.135 ± 0.015 (0.7)	4150 (3.2)
	**20**	0.90 ± 0.07	0.120 ± 0.010 (0.6)	TS[d]
$-COOCH_3$	**21**	0.70 ± 0.10	0.010 ± 0.002 (0.1)	TS[d]

[a]All values are an average of at least three independent measurements.
[b]The relative rates are given in parentheses.
[c]Determined at 37 °C.
[d]TS = too slow to measure.

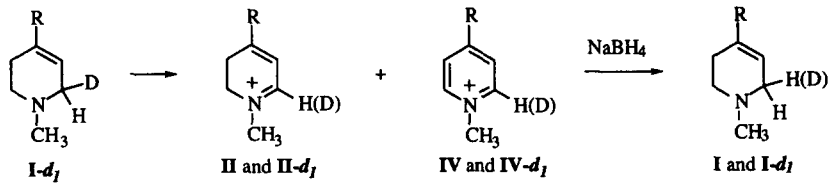

Scheme 9. Conversions associated with deuterium isotope effect studies.

Experimental

Caution: 1-Methyl-4-phenyl-1,2,3,6-tetrahydropyridine (**15**) is a known nigrostriatal neurotoxin and should be handled using disposable gloves in a properly ventilated hood. Detailed procedures for the safe handling of MPTP have been reported elsewhere.[40]

General

Reagents and starting materials were obtained from commercial suppliers and were used without further purification. Solvents were distilled under nitrogen from calcium hydride (CH_2Cl_2) and phosphorous pentoxide (MeCN). Tris(1,10-phenanthroline)iron (III)tris(hexafluorophosphate),[41] MPTP-2,2,6,6-d_4,[42] and the *N*-oxypiperidinol **47**[26] were prepared as reported previously. The hydrochloride salt of 1-methyl-4-phenyl-1,2,3,6-tetrahydropyridine (**15**) is available from Aldrich. The tetrahydropyridines **16**,[15] **17**,[16] **18**,[43] **19**,[16] **20**,[15] **21**,[44] and the dihydropyridinium species **22**,[23] **24**[16] (in the experimental part we record the corrected ^{1}NMR assignments), **26**,[16] and **27**[15] have been previously described. The free bases of the tetrahydropyridine derivatives were prepared by ethyl acetate extraction of a saturated aqueous K_2CO_3 solution of the corresponding oxalate or hydrochloride salt. All reactions were conducted under anhydrous conditions using flame-dried glassware and an atmosphere of dry nitrogen. Chromatography refers to flash column chromatography on silica gel unless otherwise noted. Melting points were performed on a Thomas–Hoover melting point apparatus and are uncorrected. Microanalyses were performed by Atlantic Microlab, Norcross, GA. ^{1}H NMR spectra were recorded on a Bruker WP 270-MHz spectrometer and ^{13}C spectra on a Varian ASM 100 400MHz spectrometer. Chemical shifts are expressed in ppm downfield from internal tetramethylsilane ($\delta = 0$). Spin multiplicities are given as s (singlet), bs (broad singlet), d (doublet), t (triplet), or m (multiplet). Coupling constants (J) values are given in hertz (Hz). GC-EIMS was performed at an ionization voltage of 70 eV on a Hewlett Packard (HP) 5890 GC, fitted with an HP-1 methyl silicone capillary column (12.5 m × 0.2 mm × 0.33 μm film thickness), which was coupled to an HP 5870 mass-selective detector and employing helium as the carrier gas (40 mL/min). Data were acquired using an HP 5970 Chemstation. Normalized peak heights are reported as a percentage of the base peak. Gas chromatography–chemical ionization mass spectroscopy (GC–CIMS) was performed on a Fisons Instrument GC 8000, fitted with a column DB-5MS (15 m × 0.25 mm × 0.25 μm film thickness), which was coupled to a Fisons Instrument Quattro mass-selective detector and employing methane as the carrier gas at the 1-torr pressure. High resolution-electron ionization mass spectroscopy (HR-EIMS) was performed on a VG 7070 HF instrument using methane as the reagent gas. UVvis absorption spectra were recorded on a Beckman DU-7000 spectrophotometer. Semiempirical calculations (AM1) were performed within MacSpartan (WaveFunction) software on an Apple PowerMac 7200/90. An unrestricted Hartree–Fock approximation was used to calculate the energy of the radicals.

Table 2. Isotope effects observed with the tetrahydropyridines **15–19**

C-4 Substituent		Isotope Effect (kH/kD)[a] SET	HAT
Ph	**15**	1.65 ± 0.07	1.91 ± 0.01
	**16**	2.00 ± 0.06	1.98 ± 0.04
–OPh	**17**	2.03 ± 0.02	2.16 ± 0.01
$-C(CH_3)_3$	**18**	2.30 ± 0.03	1.90 ± 0.02
–SPh	**19**	1.92 ± 0.08	2.14 ± 0.3

[a]All the isotope effect values are an average of at least three independent measurements.

Isotopic compositions

GC-EIMS data were collected for compounds **I-d_1** in the scan mode and the isotopic compositions were determined by measuring the abundances of *m/z* 97 relatively to *m/z* 96. The fragment ion at *m/z* 97, corresponding to the loss of the C4-substituent group of the d_1-analogue,[45] was used because of the high intensity of the peak and the low contribution of 97-1 to the *m/z* 96 ion. Corrections have been made for **15-d_1** and **18-d_1** to account for the percentage of *m/z* 95 compared to *m/z* 96 observed on the mass spectrum of the corresponding undeuterated compound. For the other undeuterated standards, the ion intensity at *m/z* 95 was below detection limits observed. Based on these analyses, the isotopic compositions **15-d_1** and **17-d_1**–**19-d_1** were estimated to be >97%. A similar analysis, only using the parent ion (also the base peak) of **16-d_1** (*m/z* 177), established the deuterium enrichment of this compound also to be >97%.

1-Methyl-4-phenoxy-2,3-dihydropyridinium perchlorate salt (24).[16b] ^{1}H NMR (DMSO-d_6) δ 3.07 (t, 2H, C_3, J = 9.4 Hz), 3.51 (s, 3H, N^+-CH_3), 3.99 (t, 2H, C_2, J = 9.4

Hz), 5.27 (d, 1H, C_5, J = 5.6 Hz), 7.24 (m, 2H, $C_{2'}$, $C_{6'}$), 7.38–7.44 (m, 1H, $C_{4'}$), 7.53–7.59 (m, 2H, $C_{3'}$, $C_{5'}$), 8.32 (d, 1H, $C_{6'}$, J = 5.6 Hz).

4-*tert*-Butyl-1-methyl-2,3-dihydropyridinium perchlorate salt (25). *m*-CPBA (50–60%, 3.11 g, 9.84 mmol) was added to a solution of 1-methyl-4-*tert*-butyl-1,2,3,6-tetrahydropyridine [free base obtained from the corresponding oxalate salt **18** (2 g, 8.2 mmol)] in dry CH_2Cl_2 (150 mL) at 0 °C. The solution was stirred at 0 °C for 1 h and the solvent was removed under reduced pressure. The crude *N*-oxide **32** in 40 mL of CH_2Cl_2 was stirred with TFAA (5.8 mL, 8.2 mmol) at 0 °C for 1 h following which the solvent was removed under reduced pressure. A solution of 70% $HClO_4$ (1.17 mL) and 10 mL of MeOH were added together with 1 mL Et_2O. The crystals obtained on cooling were recrystallized from MeOH/Et_2O to give **25** (2g, 7.4 mmol) in 90% yield: mp 121–122 °C; ^{1}H NMR (DMSO-d_6) δ 1.14 (s, 9H, *t*Bu), 2.74 (t, 2H, C_3, J = 9.3 Hz), 3.58 (s, 3H, N^+-CH_3), 3.81 (t, 2H, C_2, J = 9.4 Hz), 6.32 (d, 1H, C_5, J = 4.6 Hz), 8.45 (d, 1H, $C_{6'}$, J = 4.6 Hz). Anal. calcd for $C_{10}H_{18}ClNO_4$: C, 47.72; H, 7.21; N, 5.56; found C, 47.59; H, 7.25; N, 5.51.

Reaction of the *N*-oxypiperidinol 47 with TFAA: isolation of 1-methyl-4-(1-methyl-5-trifluoroacetyl-pyrrol-2-yl)-1,2,3,6-tetrahydropyridine (50) and 1-methyl-4-[1-methyl-5-(2′,2′,2′-trifluoro-1′-ol-ethyl)-pyrrol-2-yl)-1,2,3,6-tetra-hydropyridine (51). TFAA (1.5 mL, 7.5 mmol) was added to a solution of the *N*-oxypiperidinol **47** (300 mg, 1.5 mmol) in dry CH_2Cl_2 (10 mL) at 0 °C. The solution was stirred for 30 min and the solvent was removed under reduced pressure. To the residue was added a solution of 10% $HClO_4$ in MeOH (9 mL). The addition of a few drops of Et_2O gave **49** (320 mg, 1.16 mmol) in 78% yield as orange crystals: ^{1}H NMR (DMSO-d_6) δ 3.13 (t, 2H, C_3, J = 9.3 Hz), 3.68 (s, 3H, N^+-CH_3), 3.98 (t, 2H, C_2, J = 9.3 Hz), 4.00 (s, 3H, N-CH_3), 6.83 (d, 1H, $C_{4'}$, J = 4.6 Hz), 6.97 (d, 1H, $C_{3'}$, J = 4.6 Hz), 7.34–7.37 (m, 1H, C_5), 8.64–8.66 (m, 1H, C_6); UV (MeOH, nm); λ_{max} = 409. A solution of the unstable **49** (100 mg, 0.36 mmol) in MeOH (10 mL) was treated at 0 °C with $NaBH_4$ (19.6 mg, 0.52 mmol) portionwise. The trifluoroacetyltetrahydropyridine derivative **50**, which was formed immediately, underwent partial further reduction during the 30-min reaction period to the carbinol **51**. AcOEt extraction of the reaction mixture in saturated aqueous K_2CO_3 yielded a mixture of **50** and **51** which was separated by chromatography using CH_2Cl_2/MeOH (95/5) as eluent. The trifluoroacetyl derivative **50** eluted first and was obtained as an unstable yellow oil: ^{1}H NMR ($CDCl_3$) δ 2.41 (s, 3H, N-CH_3), 2.40–2.46 (m, 2H, C_3), 2.65 (t, 2H, C_2, J = 5.7 Hz), 3.13 (A part of an ABX, 1H, C_6, J_{AB} = 2.9 Hz), 3.15 (B part of an ABX, 1H, C_6, J_{AB} = 2.9 Hz), 3.89 (s, 3H, N-CH_3), 5.88–5.90 (m, 1H, C_5), 6.16 (d, 1H, $C_{3'}$, J = 4.4 Hz), 7.16–7.20 (m, 1H, $C_{4'}$); GC-EIMS (free base, *m/z*, %) 273 (46), 272 ($M^{\cdot+}$, 100), 271 (52), 243 (17), 203 (17), 190 (26), 175 (20), 160 (39), 132 (22), 96 (26), 94 (28), 70 (15). The second fraction gave the carbinol **51** as a yellow solid: ^{1}H NMR ($CDCl_3$) δ 2.22–2.24 (m, 2H, C_3), 2.31 (s, 3H, N-CH_3), 2.44–2.51 (m, 1H, C_2), 2.63–2.69 (m, 1H, C_2), 2.88 (A part of an ABX, 1H, C_6, J_{AB} = 16.8 Hz, J_{AX} = 2.8 Hz), 3.07 (B part of an ABX, 1H, C_6, J_{AB} = 16.8 Hz), 3.56 (s, 3H, N-CH_3), 4.25 (bs, 1H, OH), 4.94 (q, 1H, CH(OH)CF_3, J_{H-F} = 6.9 Hz), 5.42 (bs, 1H, C_5), 5.95 (d, 1H, $C_{3'}$, J = 3.8 Hz), 6.20 (bs, 1H, $C_{4'}$); ^{13}C NMR ($CDCl_3$) δ 29.3, 32.5, 45.4, 51.9, 66.5 (q, J_{C-F} = 130.4 Hz), 106.5, 107.7, 122.7, 126.1, 127.0, 127.2, 136.2; GC-EIMS (free base, *m/z*, %) 274 ($M^{\cdot+}$, 100), 273 (70), 245 (24), 192 (20), 175 (20), 162 (24), 132 (15), 94 (24), 70 (15). EI-HRMS: calcd for $C_{13}H_{17}F_3N_2O$: 274.1293 (M^+); found: 274.1296. The deuterated analogues **50-*d*$_1$** and **51-*d*$_2$** were obtained with $NaBD_4$: 1-methyl-4-(6-deutero-1-methyl-5-trifluoroacetylpyrrol-2-yl)-1,2,3,6-tetrahydropyridine (**50-*d*$_1$**) was isolated as an unstable yellow oil: ^{1}H NMR ($CDCl_3$) δ 2.40 (s, 3H, N-CH_3), 2.40–2.45 (m, 2H, C_3), 2.62–2.67 (m, 2H, C_2), 3.09–3.12 (m, 1H, C_6), 3.89 (s, 3H, N-CH_3), 5.88–5.89 (m, 1H, C_5), 6.16 (d, 1H, $C_{3'}$, J = 4.5 Hz), 7.16–7.19 (m, 1H, $C_{4'}$); GC-EIMS (free base, *m/z*, %) 273 ($M^{\cdot+}$, 100), 272 (65), 271 (22), 244 (20), 204 (15), 190 (20), 176 (17), 161 (39), 133 (15), 97 (13), 95 (11). 1-Methyl-4-[6-deutero-1-methyl-5-(2′,2′,2′-trifluoro-1′-deutero-1′-ol-ethyl)-pyrrol-2-yl)-1,2,3,6-tetrahydropyridine (**51-*d*$_2$**) was isolated as a yellow solid: ^{1}H NMR ($CDCl_3$) δ 2.21–2.23 (m, 2H, C_3), 2.30 (s, 3H, N-CH_3), 2.40–2.51 (m, 1H, C_2), 2.60–2.70 (m, 1H, C_2), 2.85 (bs, 1/2 H, C_6), 3.03 (bs, 1/2 H, C_6), 3.56 (s, 3H, N-CH_3), 5.41 (bs, 1H, C_5), 5.95 (d, 1H, $C_{3'}$, J = 3.8 Hz), 6.19–6.21 (m, 1H, $C_{4'}$); GC-EIMS (free base, *m/z*, %) 276 ($M^{\cdot+}$, 100), 275 (65), 274 (22), 247 (24), 193 (17), 176 (22), 164 (33), 133 (17), 95 (41), 71 (17). EI-HRMS: calcd for $C_{13}H_{15}D_2F_3N_2O$: 276.1419 (M^+); found: 274.1414.

General procedure for the synthesis of the oxalate salts of the 1-methyl-4-substituted-1,2,3,6-tetrahydropyridine-6-*d*$_1$ (I-*d*$_1$) substrates. The undeuterated tetrahydropyridine derivatives (**I**) were converted to the *m*-chlorobenzoate salts of the corresponding *N*-oxides (**III**) with 1 equiv of *m*-CPBA in CH_2Cl_2 at 0 °C. The free *N*-oxides, obtained by filtering the salts through a column of basic alumina with CH_2Cl_2 containing 1–5% MeOH, were stirred with an excess of TFAA in CH_2Cl_2 at 0 °C for 30 min. The solvent was removed and the resulting dihydropyridinium products (**II**) in MeOH were reduced with a 2 mol excess of $NaBD_4$ at 0 °C. After removing the solvent, a saturated solution of K_2CO_3 was added and the resulting mixture was extracted with AcOEt to isolate the monodeuterated tetrahydropyridines **I-*d*$_1$** as their free bases which were purified as the corresponding oxalate salts. The physicochemical and spectroscopic properties of these compounds were essentially identical to those of the corresponding undeuterated starting materials except for those features relating to the deuterium atom.

Kinetic studies employing the SET model

A mixture of MPTP free base (12.5 μmol) and the free base of **17**, **18**, **19**, or **21** (12.5 μmol) in 10 mL MeCN containing pyridine (5 μL, 62.5 μmol) was treated with tris(1,10-phenanthroline)iron(III)tris(hexafluorophos-

phate) (22.95 mg, 22.5 μmol) at room temperature. After stirring for 15 min, three 0.6 mL aliquots of the reaction mixture were taken. The 4-(4-pyridyl)tetrahydropyridine analogue **20** was examined in the same way except that the reaction was run in 30 mL of MeCN and 1.2 mL aliquots were taken after a 10-min reaction period. Each of these aliquots was treated with a solution of $NaBD_4$ (4.9 mg, 118 μmol) in MeOH (1 mL). After 30 min, the solvent was evaporated under reduced pressure and saturated solution of K_2CO_3 (1 mL) was added. The aqueous solution was extracted with Et_2O (0.7 mL) and the organic phase was dried over $MgSO_4$ and analyzed by GC-EIMS in the scan mode. Except for the 4-phenoxytetrahydropyridine analogue **17**, the following GC temperature program was used: 60 °C for 2 min and followed by a ramp of 25 °C/min up to 290 °C. For compound **17** separation from MPTP was achieved with the following temperature program: 60 °C for 2 min followed by three ramps −25 °C/min to 144 °C, 1 °C/min to 146 °C and finally 60 °C/min to 290 °C. The extent of conversion of the individual tetrahydropyridine analogues and MPTP into the corresponding dihydropyridinium metabolites was determined from the peak heights at *m/z* 96 and *m/z* 97, which correspond to the fragment ions of the d_0 and d_1 compounds derived from loss of the C-4 substituent (see earlier discussion concerning correction required for peak height measurements for **15** and **18**). The relative rates of oxidation of **17–19** and **21** to MPTP (**15**) were then calculated from equation 1. In a similar way, the reactivity of the 4-(1-methylpyrrol-2-yl)tetrahydropyridine analogue **16** was compared to that of the 4-(4-pyridyl)tetrahydropyridine **20** because **16** and MPTP could not be resolved on GC. The three aliquots (1.2 mL each) were taken at 10 min and were analyzed by GC-EIMS using the single ramp temperature program. The extent of conversion of **16** to the corresponding dihydropyridinium metabolite **23** was determined from the parent peak intensities at *m/z* 176 and *m/z* 177 since **16** does not give a fragment ion at *m/z* 96. It was necessary to take into account the M-1 peak (*m/z* 176, 54% of the *m/z* 177 peak) coming from **16-d_1** and the satellite M+1 peak (*m/z* 177, 12.5% of *m/z* 176) coming from **16**.

Kinetic studies employing the HAT model

To a solution of each of the tetrahydropyridine analogues (**I**, free base, 114 μmol) and CuCl (1.1 mg, 11 μmol) in MeCN (5 mL) was added at room temperature *tert*-butyl peroxybenzoate (0.1 mL, 0.57 mmol). Aliquots (0.1 mL) of the reaction mixture, taken every min for 10 min, were treated with an excess of $NaBD_4$ in MeOH. After 30 min, the solvent was evaporated under reduced pressure and saturated solution of K_2CO_3 (1 mL) was added. The aqueous solution was extracted with AcOEt (1 mL) and the organic phase was dried over $MgSO_4$ and analyzed by GC-EIMS using, in most cases, the following GC temperature program: 90 °C for 2 min followed by a ramp of 25 °C/min to 290 °C. Since **18** and **21** are more volatile, the temperature program started at 60 °C. The extent of conversion of the tetrahydropyridine substrates **I** to the corresponding pyridinium products **IV** was determined for compounds **15** and **17–21** by integration of the peaks *m/z* 96 and *m/z* 98 (taking into account the contribution of 98-2 to *m/z* 96) and for compound **16** by integration of the parent peaks *m/z* 176 and *m/z* 178 corresponding to compounds **16** and **16-d_2**. The straight-line plot of the logarithm of the concentration of **I-d_2** as a function of time gave estimates of the apparent reaction rate for each tetrahydropyridine substrates.

Isotope effect studies under SET conditions

The free base forms of the tetrahydropyridine analogues **15-d_1** and **17-19-d_1** (12.5 μmol)] were dissolved in 50 mL of dry CH_2Cl_2. Pyridine (5 μL, 62.5 μmol) was added followed by tris(1,10-phenanthroline)iron(III) tris(hexafluorophosphate) (126.9 mg, 0.123 mmol). The solution color turned from blue to red. After stirring the mixture at room temperature for 12 h, three 2 mL aliquots of the reaction mixture were taken and treated with a solution of $NaBH_4$ (4.4 mg, 118 μmol) in MeOH (1 mL). The reaction mixtures, which were worked-up as described above for the SET kinetic studies, were analyzed by GC-EIMS using the selected ion monitoring mode. The isotope effect (k_H/k_D) estimates were taken to be equal to the ratios of abundances d_0/d_1 (peak intensities at *m/z* 96/97). Some corrections were made taking to account for the contribution of *m/z* 97-1 to the *m/z* 96 when required (see earlier discussion on SET kinetic studies for details). In the case of the pyrrolyl analogue **16**, the incubations contained 50 mg (50 μmol) of tris(1,10-phenanthroline)iron(III) tris(hexafluorophosphate) in 25 mL of CH_2Cl_2 and 4 mL aliquots were taken. After work-up, the isotope effect (k_H/k_D) was estimated as the ratio of the abundances of d_0/d_1 (parent ion intensities at *m/z* 176/177) with the appropriate corrections.

Isotope effect studies under HAT conditions

To a solution of each of the tetrahydropyridine free bases **15-d_1–19-d_1** (114 μmol) and CuCl (1.1 mg, 11 μmol) in MeCN (5 mL) was added at room temperature *tert*-butyl perbenzoate (0.1 mL, 0.57 mmol). After stirring the mixture for 12 h at room temperature, 50 μL aliquots were taken and quenched with a solution of $NaBH_4$ (2 mg, 50 μmol) in MeOH (1 mL). The solutions were treated and analyzed as described above in the corresponding kinetic study.

Disproportionation study under SET conditions

A solution of the free bases of the MPTP-d_0 (7.5 μmol) and MPTP-2,2,6,6-d_4 (17.5 μmol)] in 10 mL of dry CH_2Cl_2 containing pyridine (0.25 mmol) was treated with tris(1,10-phenanthroline)iron(III)tris(hexafluoro-

phosphate) (0.1 mmol). Aliquots (0.6 mL) taken just before and at t = 5, 10, 15, 30, 45, and 75 min following the addition of the iron reagent were worked-up as described for the other SET studies and were analyzed by GC-EIMS using the scan mode. The extent of disproportionation was estimated by the intensity of the m/z 99 peak, due to the M-C_6H_5 fragment of **15-d_3** which, at t = 0, was not detectable and which increased throughout the reaction period.

Disproportionation study under HAT conditions

To a solution of MPTP-d_0 (34.5 μmol) and MPTP-2,2,6,6-d_4 (80.5 μmol)] in MeCN (5 mL) were added at room temperature CuCl (1.1 mg, 11 μmol) and *tert*-butyl peroxybenzoate (0.57 mmol). Aliquots (0.1 mL) of the reaction mixture, taken just before and then, following the addition of the *tert*-butyl peroxybenzoate, up to 25 min were worked-up and analyzed for the presence of MPTP-d_3 which was not detected in any of the samples.

Acknowledgements

This work was supported by the National Institute of Neurological and Communicative Disorders and Strokes (NS 28792) and by the Harvey W. Peters Center for the Study of Parkinson's Disease. S.M. is the recipient of a Lavoisier fellowship awarded by the Ministère des Affaires Etrangères, France. The authors thank Dr Amit Kalgutkar for the synthesis of **25**.

References

1. Kuhn, D. M.; Murphy, D. L.; Youdin, M. B. H. In *Physiological and Clinical Aspects of Monoamine Oxidase. Structure and Function of Amine Oxidases*; Kuhn, D. M.; Murphy, D. L.; Youdin, M. B. H., Eds.; CRC: Boca Raton, 1985; Vol 22, p 231.

2. Green, A. R.; Mitchell, B.; Tordoff, A.; Youdim, M. B. H. *Br. J. Pharmacol.* **1977**, 60, 343.

3. McEwen, C. M.; Sasaki, G.; Jones, D. C. *Biochemistry* **1969**, 8, 3952.

4. Dosert, P.; Strolin Benedetti, M.; Tipton, K. F. *Med. Res. Rev.* **1989**, 9, 45.

5. Kim, J.-M.; Bogdan, M. A.; Mariano, P. S. *J. Am. Chem. Soc.* **1993**, 115, 10591.

6. Silverman, R. B.; Zelechonok, Y. *J. Org. Chem.* **1992**, 57, 6373.

7. Silverman, R. B.; Yamasaki, R. B. *Biochemistry* **1984**, 23, 1322.

8. Silverman, R. B.; Zieske, P. A. *Biochemistry* **1985**, 24, 2128.

9. Silverman, R. B.; Zieske, P. A. *Biochemistry* **1986**, 25, 341.

10. Silverman, R. B.; Lu, X. *J. Am. Chem. Soc.* **1994**, 116, 4129.

11. Kim, J.-M.; Bogdan, M. A.; Mariano, P. S. *J. Am. Chem. Soc.* **1991**, 113, 9251.

12. Yelekci, K.; Lu, X.; Silverman, R. B. *J. Am. Chem. Soc.* **1989**, 111, 1138.

13. Walker, M. C.; Edmondson, D. E. *Biochemistry* **1994**, 33, 7088.

14. Kuttab, S.; Kaltutkar, A.; Castagnoli, N., Jr. *Chem. Res. Toxicol.* **1994**, 7, 740.

15. Nimkar, S. K.; Anderson, A.; Rimoldi, J. M.; Stanton, M.; Castagnoli, K. P.; Mabic, S.; Wang, Y.-X.; Castagnoli, Jr. N. *Chem. Res. Toxicol.* **1996**, 9, 1013.

16. (a) Kalgutkar, A. S.; Castagnoli, K.; Hall, A.; Castagnoli, Jr. N. *J. Med. Chem.* **1994**, 37, 944; (b) Zhao, Z.; Dalvie, D.; Naiman, N.; Castagnoli, K.; Castagnoli, Jr. N., *J. Med. Chem.* **1992**, 35, 4473.

17. Hall, L.; Murray, S.; Castagnoli, K.; Castagnoli, Jr. N. *Chem. Res. Toxicol.* **1992**, 5, 625.

18. Anderson, A.; Kalgutkar, A.; Castagnoli, Jr. N. *Biochemistry* **1996**, 35, 3335.

19. Rimoldi, J. M.; Wang, Y.-X.; Nimkar, S. K.; Kuttab, S. H.; Anderson, A. H.; Burch, H.; Castagnoli, Jr. N. *Chem. Res. Toxicol.* **1995**, 8, 703.

20. Maeda, Y.; Ingold, K. U. *J. Am. Chem. Soc.* **1980**, 102, 328; Musa, O. M.; Horner, J. H.; Shahin, H.; Newcomb, M. *J. Am. Chem. Soc.* **1996**, 118, 3862.

21. Guengerich, F. P.; Yun, C.-H.; MacDonald, L. T. *J. Biol. Chem.* **1996**, 271, 27321.

22. Karki, S. B.; Dinnocenzo, J. P.; Jones, J. P.; Korzekwa, K. R. *J. Am. Chem. Soc.* **1995**, 117, 3657.

23. Gessner, W.; Brossi, A.; Shen, R.-S.; Fritz, R. R.; Abell, C. W. *Helv. Chem. Acta* **1984**, 67, 2037.

24. Kalgutkar, A. S.; Castagnoli, N., Jr. *J. Med. Chem.* **1992**, 35, 4165.

25. Polonovski, M. *Bull. Soc. Chim.* **1927**, 41, 1186.

26. Bai, H. Ph.D. thesis, Virginia Tech, 1991.

27. Moore, G. R.; Williams, R. J. P. *Coord. Chem. Rev.* **1976**, 18, 125.

28. Mann, C. K.; Barnes, K. K. In *Amines, Amides, and Ammonium Salts*; Bard, A. J., Ed.; Marcel Dekker: New York, 1970, p 279.

29. Loveland, J. W.; Dimeler, G. R. *Anal. Chem.* **1961**, 33, 1196.

30. Korytowski, W.; Felix, C. C.; Kalyanarama, B. *Biochem. Biophys. Res. Commun.* **1987**, 147, 354.

31. Peterson, L. A.; Caldera, P. S.; Trevor, A.; Chiba, K.; Castagnoli, Jr. N. *J. Med. Chem.* **1985**, 28, 1432.

32. Kharasch, M. S.; Fono, A. *J. Org. Chem.* **1958**, 23, 324; Kharasch, M. S.; Sosnovsky, G. *J. Am. Chem. Soc.* **1958**, 80, 756.

33. Sosnovsky, G. *Angew. Chem. Internat.* **1964**, 3, 269; Easton, C. J.; Love, S. G.; Wang, P. *J. Chem. Soc. Perkin Trans.* 1 **1990**, 277.

34. Kochi, J. K. *J. Am. Chem. Soc.* **1962**, 84, 3271; Kochi, J. K. *Tetrahedron* **1962**, 18, 483; Kochi, J. K.; Mains, H. E. *J. Org. Chem.* **1964**, 30, 1862; Kochi, J. K.; Subramanian, R. V. *J. Am. Chem. Soc.* **1965**, 87, 4855; Kochi, J. K. *Science* **1967**, 155, 415; Kochi, J. K.; Bemis, A. *Tetrahedron* **1968**, 24, 5099.

35. Kochi, J. K. *J. Am. Chem. Soc.* **1963**, 85, 1958.

36. Chacon, J. N.; Chedekel, M. R.; Land, E. J.; Truscott, T. G. *Biochem. Biophys. Res. Commun.* **1989**, 158, 63.

37. Akiyama, K.; Tero-Kubota, S.; Ikegami, Y. *J. Am. Chem. Soc.* **1983**, 105, 3601.

38. Westheimer, F. H. *Chem. Rev.* **1961**, 61, 265.

39. Dinnocenzo, J. P.; Banach, T. E. *J. Am. Chem. Soc.* **1989**, 111, 8646.

40. Pitts, S. M.; Markey, S. P.; Murphy. D. L.; Weisz, A. In *Recommended Practices for the Safe Handling of MPTP*; Markey, S. P.; Castagnoli, Jr. N.; Trevor, A. J.; Kopin, I. J., Eds.; Academic: New York, 1995, p 703.

41. Schlesener, C. J.; Amatore, C.; Kochi, J. K. *J. Am. Chem. Soc.* **1984**, 106, 3567.

42. Otroboni, S.; Caldera, P.; Trevor, A.; Castagnoli Jr., N. *J. Biol. Chem.* **1989**, 264, 13684.

43. Yougster, S. K. Thesis, State University of New Jersey: New Brunswick, 1987, p 175.

44. Bosch, J.; Rubiralta, M.; Domingo, A.; Bolos, J.; Linares, A.; Minguillon, C.; Amat, M.; Bonjoch, J. *J. Org. Chem.* **1985**, 50, 1516.

45. Mabic, S.; Castagnoli Jr., N. *J. Mass. Spectrom.*, submitted.

(*Received in U.S.A.* 6 *February* 1997; *accepted* 24 *March* 1997)